MMSE TURBO EQUALIZATION FOR MULTICODE DS-CDMA

Kazuaki TAKEDA[+] *and Fumiyuki ADACHI*[++]
Dept. of Electrical and Communication Engineering, Graduate School of Engineering, Tohoku University
6-6-05 Aza-Aoba, Aramaki, Aoba-ku, Sendai, 980-8579 Japan
E-mail: [+]takeda@mobile.ecei.tohoku.ac.jp, [++]adachi@ecei.tohoku.ac.jp

ABSTRACT

Frequency-domain equalization (FDE) based on the minimum mean square error (MMSE) criterion can replace the conventional rake combining with significantly improved bit error rate (BER) performance of multicode DS-CDMA in a frequency-selective fading channel. However, the presence of residual inter-chip-inference (ICI) after MMSE-FDE produces the orthogonality distortion among the spreading codes and the BER performance degrades as the number of multiplex order increases. Recently, we have proposed a frequency-domain ICI cancellation to improve the uncoded performance. To further improve the BER performance, in this paper, we propose MMSE turbo equalization. In the proposed scheme, MMSE-FDE and ICI cancellation are incorporated into iterative maximum *a posteriori* (MAP) decoding, resulting in an MMSE turbo equalization. MMSE weight taking into account the residual ICI is updated in each iteration. The effect of MMSE turbo equalization is confirmed by computer simulation.

Keywords-component; DS-CDMA, frequency-domain equalization, ICI cancellation, MMSE turbo equalization

1. INTRODUCTION

In the third generation mobile communication systems, direct sequence code division multiple access (DS-CDMA) is successfully used [1]. Wireless channel is composed of many distinct propagation paths having different time delays, resulting in a frequency-selective fading channel [2]. In the present cellular systems adopting DS-CDMA, rake combining is applied to combat with the frequency-selective fading channel for the data transmissions of up to around a few Mbps [1], [3]. Recently, a lot of research attention has been paid to the next generation mobile communication systems that will support data services higher than several tens of Mbps. The wireless channel for high speed data transmission is severely frequency-selective and the BER performance with the rake combining degrades due to a strong inter-path interference. Hence, an advanced equalization technique is indispensable.

Recently, it has been shown [4]-[7] that FDE based on the minimum mean square error (MMSE) criterion can replace the rake combining and improve the BER performance for the DS-CDMA signal reception over a severe frequency-selective channel. Although FDE can significantly improve the downlink BER performance, the presence of residual inter-chip interference (ICI) after FDE distorts the orthogonality among the spreading codes and the BER performance of orthogonal multicode DS-CDMA degrades as the code multiplexing order increases. The joint use of FDE and multi-access interference (MAI) cancellation for DS-CDMA uplink is considered in [8]. Recently, we have proposed a joint MMSE-FDE and frequency-domain ICI cancellation to improve the uncoded BER performance of the DS-CDMA downlink signal transmission [9].

For the data transmissions higher than 100Mbps, the use of strong error correction technique (e.g., turbo coding) is inevitable [10]. Recently, the turbo equalization technique has been drawing much attention since it can suppress the interference while achieving high coding gain by iteratively performing channel equalization and channel decoding [11]-[13]. In this paper, we propose MMSE turbo equalization to suppress the residual ICI present after FDE and to improve the decoded BER performance of multicode DS-CDMA. In the proposed scheme, MMSE-FDE, ICI cancellation and maximum *a posteriori* (MAP) decoding are repeated to successively suppress the residual ICI and to obtain the higher coding gain. MMSE weight taking into account the residual ICI is updated in each iteration.

2. TRANSMISSION SYSTEM MODEL

2.1. Overall transmission system

The transmission system model for DS-CDMA with turbo equalization is illustrated in Fig.1. At the transmitter, after turbo coding and channel interleaving, a binary data sequence of $K\log_2 M$ bits is transformed into a data modulated symbol sequence $\{d(n);\ n=0\sim K-1\}$, where M is the modulation level. The resulting data modulated symbol sequence is transformed, by serial-to-parallel (S/P) converter, into U parallel symbol sequences $\{d_u(m);\ m=0\sim K/U-1\}$, $u=0\sim U-1$, and then each sequence is divided into a sequence of blocks of N_c/SF chips. Here, N_c is the FFT window size and SF is the spreading factor. In this paper, one block transmission of $\{d_u(m);\ m=0\sim N_c/SF-1\}$ is considered for simplicity (i.e., $K/U=N_c/SF$).

One block of data symbols $\{d_u(m);\ m=0\sim N_c/SF-1\}$ is spread by multiplying an orthogonal spreading sequence $c_u(t)$ of spreading factor SF. The resultant U chip sequences are multiplexed and further multiplied by a common scramble sequence $c_{scr}(t)$ to make the resultant multicode DS-CDMA signal like white-noise. Then, the last N_g chips of each block are copied as a cyclic prefix and inserted into the guard interval (GI) at the beginning of each block.

The GI-inserted orthogonal multicode DS-CDMA signal is transmitted over a frequency-selective fading channel and is received at a receiver. After the removal of the GI, the received chip sequence is decomposed by N_c-point FFT into N_c subcarrier components (the terminology "subcarrier" is used for explanation purpose only; subcarrier modulation is not used). MMSE-FDE is carried out, then, ICI cancellation is performed in the frequency-domain. Inverse FFT (IFFT) is applied to obtain the time-domain received chip sequence for despreading. After performing channel deinterleaving and MAP decoding, the soft symbol replica is generated using the decoder output (log likelihood ratio (LLR)). This replica is fedback for MMSE weight updating and ICI replica generation. A series of MMSE-FDE, ICI cancellation, despreading and MAP decoding is repeated a sufficient number of times before obtaining the final received data.

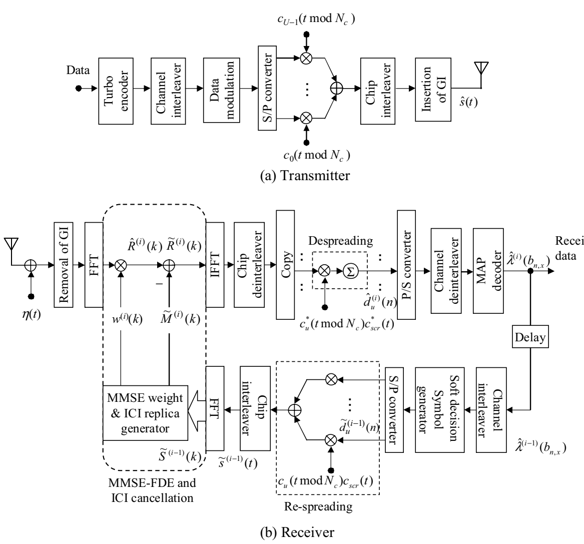

Figure 1. Transmitter/receiver structure.

2.2. Transmit and receive signals

Throughout this paper, chip-spaced time representation of the transmitted signals is used. The chip sequence $\{\hat{s}(t);\ t=-N_g\sim N_c-1\}$, to be transmitted after the GI insertion, can be expressed, using the equivalent lowpass representation, as

$$\hat{s}(t)=\sqrt{2E_c/T_c}\,s(t \bmod N_c)\ , (1)$$

where E_c and T_c denote the chip energy and the chip duration, respectively, and $s(t)$ is given by

$$s(t)=\left[\sum_{u=0}^{U-1} d_u\left(\lfloor t/SF\rfloor\right)c_u(t \bmod SF)\right]c_{scr}(t) \quad (2)$$

with $|c_u(t)|=|c_{scr}(t)|=1$ for $t=0\sim(N_c-1)$, where $\lfloor x\rfloor$ represents the largest integer smaller than or equal to x.

The propagation channel is assumed to be a frequency-selective block fading channel having chip-spaced L discrete paths, each subjected to independent fading. The assumption of block fading means that the path gains remain constant over at least one block duration. The impulse response $h(t)$ of a multipath channel can be expressed as

$$h(t)=\sum_{l=0}^{L-1} h_l\delta(t-\tau_l)\ , \ (3)$$

where h_l and τ_l are the complex-valued path gain and time delay of the lth path (l=0~L−1), respectively, with $\sum_{l=0}^{L-1}E[|h_l|^2]=1$ (E[.] denotes the ensemble average operation). The received chip sequence $\{r(t);t=-N_g\sim N_c-1\}$ can be expressed as

$$r(t)=\sum_{l=0}^{L-1} h_l\hat{s}(t-\tau_l)+\eta(t)\quad , (4)$$

where $\eta(t)$ is a zero-mean complex Gaussian process with a variance of $2N_0/T_c$ with N_0 being the single-sided power spectrum density of the additive white Gaussian noise (AWGN) process.

2.3. MMSE-FDE and ICI cancellation

A joint MMSE-FDE and ICI cancellation is repeated in an iterative fashion. Below, the ith iteration is described.

After the removal of the GI from the received chip sequence $r(t)$, N_c-point FFT is applied to decompose $\{r(t);t=0\sim N_c-1\}$ into N_c subcarrier components $\{R(k);\ k=0\sim N_c-1\}$. The kth subcarrier component $R(k)$ can be written as

$$\begin{aligned}R(k)&=\sum_{t=0}^{N_c-1} r(t)\exp\left(-j2\pi k\frac{t}{N_c}\right)\\&=H(k)S(k)+\Pi(k)\end{aligned}\ , (5)$$

where $S(k)$, $H(k)$ and $\Pi(k)$ are the kth subcarrier component of the transmitted signal sequence $\{s(t);\ t=0\sim N_c-1\}$ of N_c chips, the channel gain and the noise component due to the AWGN, respectively. They are given by

$$\begin{cases}S(k)=\displaystyle\sum_{t=0}^{N_c-1} s(t)\exp\left(-j2\pi k\frac{t}{N_c}\right)\\ H(k)=\displaystyle\sqrt{\frac{2E_c}{T_c}}\sum_{l=0}^{L-1} h_l\exp\left(-j2\pi k\frac{\tau_l}{N_c}\right)\\ \Pi(k)=\displaystyle\sum_{t=0}^{N_c-1}\eta(t)\exp\left(-j2\pi k\frac{t}{N_c}\right)\end{cases}\ . \ (6)$$

MMSE-FDE is carried out as follows:

$$\begin{aligned}\hat{R}^{(i)}(k)&=w^{(i)}(k)R(k)\\&=S(k)\hat{H}^{(i)}(k)+\hat{\Pi}^{(i)}(k)\end{aligned} \quad (7)$$

with

$$\begin{cases}\hat{H}^{(i)}(k)=w^{(i)}(k)H(k)\\ \hat{\Pi}^{(i)}(k)=w^{(i)}(k)\Pi(k)\end{cases}, (8)$$

where $w^{(i)}(k)$ is the equalization weight at the ith iteration and $\hat{H}^{(i)}(k)$ and $\hat{\Pi}^{(i)}(k)$ are respectively the equivalent channel gain and the noise component, after MMSE-FDE at the ith iteration. The equalization weight will be derived in Sect. 4.

ICI cancellation is performed as

$$\tilde{R}^{(i)}(k)=\hat{R}^{(i)}(k)-\tilde{M}^{(i)}(k) \quad , (9)$$

where $\tilde{M}^{(i)}(k)$ is the residual ICI replica, and given by [9]

$$\tilde{M}^{(i)}(k)=\begin{cases}0 & \text{for } i=0\\ \left\{\hat{H}^{(i)}(k)-A^{(i)}\right\}\tilde{S}^{(i-1)}(k) & \text{for } i>0\end{cases}, (10)$$

where $\tilde{S}^{(i-1)}(k)$ is the kth frequency component of the transmitted chip replica, which is generated by feeding back the (i–1)th ICI cancellation result and $A^{(i)}$ is given by

$$A^{(i)}=\frac{1}{N_c}\sum_{k'=0}^{N_c-1}\hat{H}^{(i)}(k'). (11)$$

N_c-point IFFT is applied to transform the frequency-domain signal $\{\tilde{R}^{(i)}(k);k=0\sim N_c-1\}$ into time-domain chip sequence $\{\tilde{r}^{(i)}(t);t=0\sim N_c-1\}$:

$$\tilde{r}^{(i)}(t)=\frac{1}{N_c}\sum_{k=0}^{N_c-1}\tilde{R}^{(i)}(k)\exp\left(j2\pi t\frac{k}{N_c}\right), \qquad (12)$$

Despreading is carried out on $\tilde{r}^{(i)}(t)$ to obtain the uth code's decision variable on $d_u(m)$, giving

$$\hat{d}_u^{(i)}(m)=\frac{1}{SF}\sum_{t=mSF}^{(m+1)SF-1}\tilde{r}^{(i)}(t)c_u^*(t \bmod SF)c_{scr}^*(t) \quad . (13)$$

3. MAP DECODING

U parallel sequences of $\{\hat{d}_u^{(i)}(m)$; m=0~N_c/SF–1}, u=0~U–1, are transformed into a sequence of $\left\{\hat{d}^{(i)}(n);n=0\sim K-1\right\}$ by parallel-to-serial (P/S) converter (i.e., $N_c/SF=K/U$). Using the soft decision variable $\left\{\hat{d}^{(i)}(n)\right\}$, the LLR $\mathbf{\Lambda}^{(i)}=\{\Lambda_0(0),..,\Lambda_0(\log_2 M-1),..,\Lambda_{K-1}(\log_2 M-1)\}$ can be computed as [14]

$$\Lambda_n(x)\approx\frac{\left|\hat{d}^{(i)}(n)-A^{(i)}d^{\min}_{b_{n,x}=0}\right|^2}{2\hat{\sigma}^2}-\frac{\left|\hat{d}^{(i)}(n)-A^{(i)}d^{\min}_{b_{n,x}=1}\right|^2}{2\hat{\sigma}^2}, (14)$$

where $b_{n,x}$ represents the xth bit in the nth symbol and $d^{\min}_{b_{n,x}=0}$ (or $d^{\min}_{b_{n,x}=1}$) is the most probable symbol that gives the minimum Euclidean distance from $\hat{d}^{(i)}(n)$ among all the candidate symbols with $b_{n,x}=0$ (or 1) and $2\hat{\sigma}^2$ is the variance of the noise plus residual ICI.

MAP decoder is illustrated in Fig. 2. In this paper, Log-MAP algorithm is used [10]. After S/P conversion, $\mathbf{\Lambda}^{(i)}$ is decomposed into three LLR sequences, $\mathbf{\Lambda}_s^{(i)}$, $\mathbf{\Lambda}_{p1}^{(i)}$ and $\mathbf{\Lambda}_{p2}^{(i)}$, associated with the information bit, 1st parity bit and 2nd parity bit, respectively. In the first MAP decoder, *a posteriori* LLR sequence $\boldsymbol{\lambda}^{(i)}=\{\lambda^{(i)}(b_{n,x});n=0\sim K-1,x=0\sim\log_2 M-1\}$ is computed, using $\mathbf{\Lambda}_s^{(i)}$, $\mathbf{\Lambda}_{p1}^{(i)}$ and *a prior* LLR $\tilde{\boldsymbol{\lambda}}_{s2}^{(i-1)}$ ($\tilde{\boldsymbol{\lambda}}_{s2}^{(i-1)}$ is obtained from the 2nd MAP decoder at the (i–1)th iteration), as [10]

$$\lambda^{(i)}(b_{n,x})=\ln\frac{p(b_{n,x}=1\mid\mathbf{\Lambda}_s^{(i)},\mathbf{\Lambda}_{p1}^{(i)})}{p(b_{n,x}=0\mid\mathbf{\Lambda}_s^{(i)},\mathbf{\Lambda}_{p1}^{(i)})}, (15)$$

where $p(b_{n,x}=1\mid\mathbf{\Lambda}_s^{(i)},\mathbf{\Lambda}_{p1}^{(i)})$ (or $p(b_{n,x}=0\mid\mathbf{\Lambda}_s^{(i)},\mathbf{\Lambda}_{p1}^{(i)})$) is the *a posteriori* probability being $b_{n,x}=1$ (or 0), given $\mathbf{\Lambda}_s^{(i)}$ and $\mathbf{\Lambda}_{p1}^{(i)}$.

The *a posteriori* LLRs $\boldsymbol{\lambda}^{(i)}$ of the information bit and parity bit are denoted by $\boldsymbol{\lambda}_{s1}^{(i)}$ and $\boldsymbol{\lambda}_{p1}^{(i)}$, respectively. After subtracting the *a prior* LLR $\tilde{\boldsymbol{\lambda}}_{s2}^{(i-1)}$ and $\mathbf{\Lambda}_s^{(i)}$ from $\boldsymbol{\lambda}_{s1}^{(i)}$, interleaving is applied to generate the *a prior* LLR $\tilde{\boldsymbol{\lambda}}_{s1}^{(i)}$ to be used for the 2nd MAP decoder. In the 2nd MAP decoder, using $\mathbf{\Lambda}_s^{(i)}$, $\mathbf{\Lambda}_{p2}^{(i)}$ and $\tilde{\boldsymbol{\lambda}}_{s1}^{(i)}$, the *a posteriori* LLRs, $\boldsymbol{\lambda}_{s2}^{(i)}$ and $\boldsymbol{\lambda}_{p2}^{(i)}$, of the information bit and the 2nd parity bit are computed. In the turbo equalization, the resulting LLRs $\boldsymbol{\lambda}_{s2}^{(i)}$, $\boldsymbol{\lambda}_{p1}^{(i)}$ and $\boldsymbol{\lambda}_{p2}^{(i)}$ are P/S converted and channel de-interleaved to generate the *a prior* LLR sequence $\hat{\boldsymbol{\lambda}}^{(i)}=\{\hat{\lambda}^{(i)}(b_{n,x});n=0\sim K-1,x=0\sim\log_2 M-1\}$, for the ($i$+1)th MMSE weight updating and ICI cancellation. $\hat{\lambda}^{(i)}(b_{n,x})$ is given by

$$\hat{\lambda}^{(i)}(b_{n,x})=\ln\left(\frac{p^{(i)}(b_{n,x}=1)}{p^{(i)}(b_{n,x}=0)}\right). (16)$$

After a series of MMSE-FDE, ICI cancellation, and MAP decoding is repeated a sufficient number of times, $\boldsymbol{\lambda}_{s2}^{(i)}$ is used for the received data recovery.

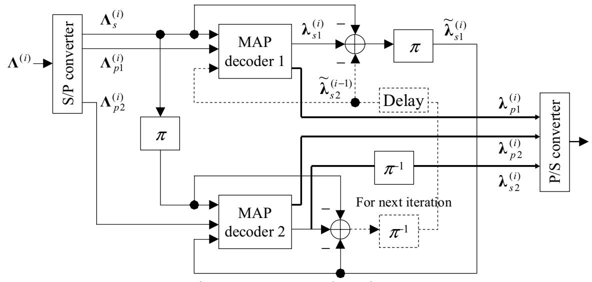

Figure 2. MAP decoder.

4. ICI REPLICA GENERATION AND MMSE WEIGHT COMPUTAION

In this section, we consider the $i(\geq 1)$th iteration. ICI replica generation for the ith iteration and the MMSE weight taking into account the residual ICI are presented.

4.1. Soft symbol replica generation

The soft decision symbol $\tilde{d}^{(i-1)}(n)$, n=0~$K-1$, can be obtained using [12]

$$\tilde{d}^{(i-1)}(n)=\sum_{d\in D} d\prod_{b_{n,x}\in d} p^{(i-1)}(b_{n,x}) \quad ,(17)$$

where d represents the candidate symbol having $b_{n,x}=0$ or $b_{n,x}=1$ in the symbol set D and $p^{(i-1)}(b_{n,x}=0)$ and $p^{(i-1)}(b_{n,x}=1)$ are given, from Eq. (16), by

$$\begin{cases} p^{(i-1)}(b_{n,x}=0)=-\dfrac{1}{2}\tanh\left(\dfrac{\hat{\lambda}^{(i-1)}(b_{n,x})}{2}\right)+\dfrac{1}{2} \\ p^{(i-1)}(b_{n,x}=1)=\dfrac{1}{2}\tanh\left(\dfrac{\hat{\lambda}^{(i-1)}(b_{n,x})}{2}\right)+\dfrac{1}{2} \end{cases} \quad (18)$$

since $p^{(i-1)}(b_{n,x}=1)+p^{(i-1)}(b_{n,x}=0)=1$.

$\tilde{d}^{(i-1)}(n)$ of Eq. (17) is the expectation of the transmitted symbol, and it is used as a soft decision symbol replica as in [12]. For QPSK data modulation, $\tilde{d}^{(i-1)}(n)$ becomes

$$\tilde{d}^{(i-1)}(n)=\frac{1}{\sqrt{2}}\tanh\left(\frac{\hat{\lambda}^{(i-1)}(b_{n,0})}{2}\right)+j\frac{1}{\sqrt{2}}\tanh\left(\frac{\hat{\lambda}^{(i-1)}(b_{n,1})}{2}\right) \quad .(19)$$

After S/P conversion to transform $\tilde{d}^{(i-1)}(n)$ into U parallel sequences of { $\tilde{d}_u^{(i-1)}(m)$; m=0~N_c/SF}, u=0~U–1, the replica $\{\tilde{s}^{(i-1)}(t);t=0\sim N_c-1\}$ of the transmitted chip sequence $s(t)$ is generated as

$$\tilde{s}^{(i-1)}(t)=\left[\sum_{u=0}^{U-1}\tilde{d}_u^{(i-1)}\left(\lfloor t/SF\rfloor\right)c_u(t \bmod SF)\right]c_{scr}(t) \quad .(20)$$

Then, N_c-point FFT is applied to decompose the replica $\tilde{s}^{(i-1)}(t)$ into N_c subcarrier components $\{\tilde{S}^{(i-1)}(k)$;k=0~(N_c–1)} as

$$\tilde{S}^{(i-1)}(k)=\sum_{t=0}^{N_c-1}\tilde{s}^{(i-1)}(t)\exp\left(-j2\pi k\frac{t}{N_c}\right) \quad .(21)$$

Substituting Eq. (21) into Eq. (10), we obtain the frequency-domain ICI replica $\tilde{M}^{(i)}(k)$.

4.2. MMSE Weight

At the first iteration (i=0), MMSE-FDE is performed before ICI cancellation. Since the residual ICI is suppressed after ICI cancellation, the MMSE weight needs to be updated in each iteration (i>0) [9]. In this paper, the MMSE weight, taking into account the residual ICI, is derived for each iteration. To derive the MMSE weight, we define the equalization error $e(k)$ between the frequency component $\{\tilde{R}^{(i)}(k);k=0\sim N_c-1\}$ after ICI cancellation and the transmitted frequency component $\{S(k);k=0\sim N_c-1\}$ as

$$e(k)=\tilde{R}^{(i)}(k)-A^{(i)}S(k) \quad ,(22)$$

where $A^{(i)}S(k)$ is used as a reference signal since $E[\tilde{R}^{(i)}(k)]=A^{(i)}S(k)$ (the residual ICI is assumed to be zero-mean). $w^{(i)}(k)$ is the weight that minimizes the mean square error (MSE) $E[|e(k)|^2]$ for the given $H(k)$, i.e., $\partial E[|e(k)|^2]/\partial w^{(i)}(k)=0$. Hence, the following MMSE weight is obtained:

$$w^{(i)}(k)=\frac{H^*(k)}{|H(k)|^2\rho^{(i-1)}+2\sigma^2} \quad , (23)$$

where $2\sigma^2$ is a noise variance of $2N_0/T_c$ and $\rho^{(i-1)}$ is an interference factor, given by

$$\rho^{(i-1)}=\sum_{t=0}^{N_c-1}\left\{|s(t)|^2-|\tilde{s}^{(i-1)}(t)|^2\right\}. \quad (24)$$

Since $s(t)$ is unknown, we use the hard decision chip sequence replica $\bar{s}^{(i-1)}(t)$ instead of $s(t)$ in Eq. (24).

5. COMPUTER SIMULATION

A turbo encoder with (13,15) RSC encoders and a decoder with Log MAP algorithm are used. A R=1/2-rate turbo code with a constraint length of 4 is assumed. The length of the coded bit sequence is $K\log_2 M$=2048 bits. We assume QPSK data modulation and 16QAM, an FFT block size of N_c=256 chips and a GI of N_g=32 chips. The channel is assumed to be a frequency-selective block Rayleigh fading channel having a chip-spaced L-path uniform power delay profile (i.e., $E[|h_l|^2]$=1/L for all l).

Perfect chip timing and ideal channel estimation are assumed. The number of iterations in the turbo equalization is assumed to be 6.

The simulated BER performance of DS-CDMA with the MMSE turbo equalization is plotted in Fig. 3 for $SF=U=1$ and 16 as a function of the average received bit energy-to-AWGN noise power spectrum density ratio E_b/N_0, defined as $E_b/N_0=(1/\log_2 M)SF(E_c/N_0)(1+N_g/N_c)$. For comparison, the BER performances of OFDM and DS-CDMA without ICI cancellation are also plotted with a turbo decoding of 6 iterations. It can be seen from Fig. 3 (a) that DS-CDMA with the MMSE turbo equalization gives better BER performance than DS-CDMA without ICI cancellation and OFDM, since the MMSE turbo equalization can successively suppress the residual ICI while achieving a higher coding gain. The same BER performance can be seen for SF=1 and 16. For 16QAM (Fig. 3 (b)), the Euclidean distance between different symbols is shorter and hence, decision error due to the residual ICI is more likely than for QPSK. Without MMSE turbo equalization (i.e., no ICI cancellation), the BER performance of DS-CDMA is worse than that of OFDM. However, the MMSE turbo equalization is very effective to improve the BER performance of DS-CDMA. The E_b/N_0 reduction from without ICI cancellation is as much as 1.9 dB for BER=10^{-4}.

6. CONCLUSION

In this paper, MMSE turbo equalization was proposed, in which ICI cancellation is incorporated into iterative turbo decoding. The MMSE weight taking into account the residual ICI was used. The coded BER performance with MMSE turbo equalization was evaluated by computer simulation. It was found that the MMSE turbo equalization can improve the coded BER performance of DS-CDMA and gives similar BER performance to OFDM since the MMSE turbo equalization can suppress the residual ICI while achieving the higher coding gain. For QPSK (16QAM), the E_b/N_0 reduction from without ICI cancellation is as much as 0.9 (1.9) dB for BER=10^{-4}.

7. REFERENCES

[1] F. Adachi, M. Sawahashi, and H. Suda, "Wideband DS-CDMA for next generation mobile communications systems," IEEE Commun. Mag., vol. 36, pp.56-69, Sept. 1998.

[2] W. C., Jakes Jr., Ed., *Microwave mobile communications*, Wiley, New York, 1974.

[3] J. G. Proakis, *Digital communications*, 3rd ed., McGraw-Hill, 1995.

[4] F. W. Vook, T. A. Thomas, and K. L. Baum, "Cyclic-prefix CDMA with antenna diversity," Proc. IEEE VTC 2002 Spring, pp. 1002-1006, May 2002.

[5] F. Adachi, T. Sao, and T. Itagaki, "Performance of multicode DS-CDMA using frequency domain equalization in a frequency selective fading channel," Electronics Letters, Vol. 39, pp.239-241, Jan. 2003.

[6] F. Adachi and K. Takeda, "Bit error rate analysis of DS-CDMA with joint frequency-domain equalization and antenna diversity combining," IEICE Trans. Commun., Vol. E87-B, pp. 2991-3002, Oct. 2004.

[7] I. Martoyo, G. M.A. Sessler, J. Luber and F. K. Jondral, "Comparing equalizers and multiuser detections for DS-CDMA downlink systems," Proc. IEEE VTC 2004-Spring, 17-19 May 2004.

[8] S. Tomasin and N. Benvenuto, "Frequency-domain interference cancellation and nonlinear equalization for CDMA systems," IEEE Trans. Wireless Commun., vol. 4, no. 5. pp. 2329-2339, Sept. 2005.

[9] K. Takeda, K. Ishihara, and F. Adachi, "Downlink DS-CDMA transmission with joint MMSE equalization and ICI cancellation," Proc. IEEE VTC 2006-Spring, 7-10 May 2006.

[10] J. P.Woodard and L. Hanzo, "Comparative study of turbo decoding techniques: An overview", IEEE Trans. Veh. Technol., Vol.49, pp.2208-2233, Nov. 2000.

[11] D. Raphaeli and Y. Zarai, "Combined turbo equalization and turbo decoding," IEEE Commun. Letters, Vol. 2, No. 2, pp. 107-109, April 1998.

[12] X. Wang and H. V. Poor, "Iterative (turbo) soft interference cancellation and decoding for coded CDMA," IEEE Commun. Mag., Vol. 47, No.7, pp.1046-1060, July 1999.

[13] C. Laot, R. L. Bidan, and D. Leroux, "Low-complexity MMSE Turbo Equalization: a possible solution for EDGE," IEEE. Trans. Wire. Commun., Vol. 4, No. 3, pp.965-974, May 2005.

[14] A. Stefanov and T. Duman, "Turbo coded modulation for wireless communications with antenna diversity," Proc. IEEE VTC99-Fall, pp.1565-1569, Netherlands, 19-22 Sept. 1999.

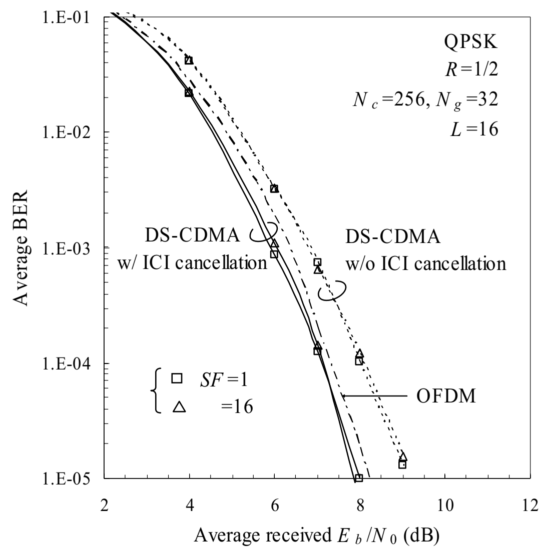

(a) QPSK

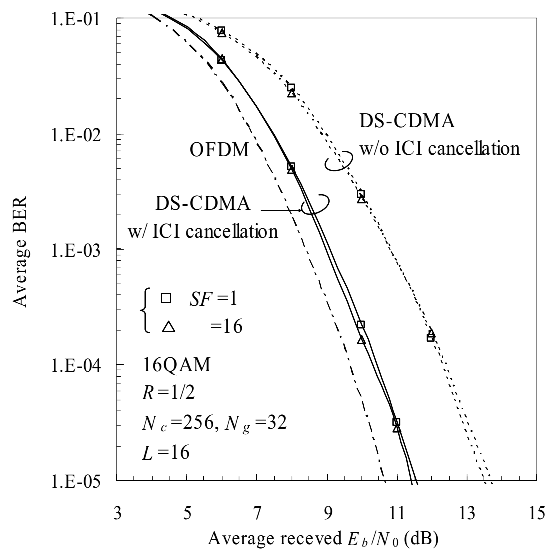

(b) 16QAM

Figure 3. Simulated BER performance with MMSE turbo equalization.